



Obrabotka metallov -

Metal Working and Material Science

Journal homepage: http://journals.nstu.ru/obrabotka_metallov







Impact of print orientation on wear behavior in FDM printed PLA Biomaterial: Study for hip-joint implant

Yogiraj Dama^{1, a, *}, Bhagwan Jogi^{1, b}, Raju Pawade^{1, c}, Atul Kulkarni^{2, d}

¹ Dr. Babasaheb Ambedkar Technological University, Lonere, Raigad, Maharashtra, 402103, India

² Vishwakarma Institute of Information Technology, Survey No. 3/4, Kondhwa (Budruk), Maharashtra, Pune - 411048, India

^a  <https://orcid.org/0009-0008-5404-4347>,  yogirajdama@dbatu.ac.in; ^b  <https://orcid.org/0000-0003-2099-7533>,  bfjogi@dbatu.ac.in;

^c  <https://orcid.org/0000-0001-7239-625X>,  rspawade@dbatu.ac.in; ^d  <https://orcid.org/0000-0002-6452-6349>,  atul.kulkarni@viit.ac.in

ARTICLE INFO

Article history:

Received: 18 August 2024

Revised: 10 September 2024

Accepted: 17 September 2024

Available online: 15 December 2024

Keywords:

3D Printing

Biomaterials

FDM

Implant

Print orientation

PLA

Wear behavior

ABSTRACT

Introduction: hip joint replacement surgery involves replacing the damaged joint with an implant that can re-create the joint's articulation functionality. 3D printing technology is more promising than the traditional manufacturing process when it comes to producing more complex parts and shapes. The goal of the current research project is to determine how quickly biomaterial implant can be manufactured using 3D printing for hip-joint replacement by studying the wear rate of parts manufactured using different printing orientations. Although there are several additive manufacturing technologies, fuse deposition modeling (FDM) technology has had a significant impact on healthcare, automotive industry, etc. This is mainly due to the adaptability of different polymer-based composite materials and its cost-effectiveness. Such 3D printed polymers need to be further studied to evaluate the wear rate depending on different 3D printing orientations. Polylactic acid (PLA) biomaterials were extensively studied to determine its suitability for use as hip joint materials. **Purpose of the work:** in this work, an experimental study was carried out on the effect of printing orientation on dry sliding wear of a polylactic acid (PLA) material obtained by fused deposition modeling (FDM) technology using the pin-on-disk (SS 316) scheme. In addition, experimental and empirical models are developed to predict the performance taking into account the influence of load and sliding speed. Grey relational analysis was used to determine the optimal parameters. **The methods of investigation:** the FDM printing was used to manufacture pins using different printing orientations. Printing direction refers to printing at angles of 0°, 45°, and 90°, while all other 3D printing parameters remained unchanged. Wear testing was performed using the pin-on-disk kinematic scheme. During the experiments, the normal pin load and disk rotation speed were varied. The experiments were methodically designed to study the effect of input parameters on the specific wear rate. About 13 experiments were conducted for each printing orientation with a friction path of 4 kilometers, in the load range of 400–800 N, at a sliding speed of 450–750 rpm. **Result and discussion:** the study provides important results especially regarding the direction of 3D printing of components. It was found that the lowest sliding wear was observed for the pin printed at an angle of 0°, while slightly higher wear was observed for the pin printed at an angle of 90°. The layer bonding in the pin printed at an angle of 45° deformed under higher load, mainly due to an increase in temperature. The low bond strength in the pin printed at an angle of 45° resulted in high sliding wear. The optimal result was achieved at a sliding speed of 451 rpm and a load of 600 N. The results of the study are very useful for choosing materials for 3D printing of biomedical implants, medical and industrial products.

For citation: Dama Y.B., Jogi B.F., Pawade R., Kulkarni A.P. Impact of print orientation on wear behavior in FDM printed PLA Biomaterial: Study for hip-joint implant. *Obrabotka metallov (tekhnologiya, oborudovanie, instrumenty) = Metal Working and Material Science*, 2024, vol. 26, no. 4, pp. 19–40. DOI: 10.17212/1994-6309-2024-26.4-19-40. (In Russian).

Introduction

In the medical domain, researchers are constantly trying to find alternative biomaterials and manufacturing processes [1]. For the creation of more complex parts and shapes, 3D printing technology is more promising than conventional manufacturing methods. The 3D printing process, also called as additive

* Corresponding author

Dama Yogiraj Basavraj, Research Scholar

Dr. Babasaheb Ambedkar Technological University,

Lonere, Raigad,

402103, Maharashtra, India

Tel.: +91-9860384360, e-mail: yogirajdama@dbatu.ac.in

manufacturing process, has found wide application in the engineering domain, especially for the design of complex components and on-demand printing [2]. However, this technology has not yet proven itself in the medical domain due to many limitations such as availability of 3D printing biomaterials, printing orientations, regulatory approval, long-term reliability and the use of printed products in the patient's body in real time etc., so researchers have focused on the use of 3D printing process for medical domain [1].

The hip-joint, and therefore the hip implant, is one of the most critical joints in the human body compared to any other joint. Despite significant progress in the development of hip implants using various biomaterials including metal, ceramic and polymers, there is still much room for research and development of customized hip implants, even though biomaterials and hip replacement techniques have come a long way over the past few centuries. The hip joint connects the femoral bone to the pelvis, supporting the entire weight of the human body. The hip joint is one of the most important joints supporting the human body. The natural location of the acetabulum is a cup-shaped cavity into which the smooth spherical head of the femur fits precisely and subsequently slides. Strong ligaments surround the entire joint, providing stability. Innovations in design and materials over the last 50 years have significantly reduced the actual wear rate of the most popular implants, which in turn allows us to significantly reduce the risks associated with widespread dissemination of debris throughout the human body.

Biomaterials such as ultra-high molecular weight polyethylene (*UHMWPE*), high-density polyethylene (*HDPE*), polyetheretherketone (*PEEK*) and others are commonly used in medicine for implant manufacture in a traditional way and are well proven [3–4]. *Lewis* [5] studied the properties of crosslinked ultra-high-molecular-weight polyethylene. *Wang et al.* found that the lubricity and wear properties of polyethylene in total joint replacement are improved [6]. *Yousuf and Mohsin* [7] studied the increase in the wear rate of high-density *HDPE* by adding ceramic particles. However, implanted polyethylene acetabular cups generate debris, which is reacted to by the body's immune system [8]. To improve the mechanical and tribological characteristics of the *HDPE* matrix, nanocomposites including graphene, TiO_2 nanoparticles and hybrid nanofillers were added to it, which ultimately led to an increase in service life and a decrease in wear rate [9].

Zhang et al. [10] observed the use of *PEEK* as an alternative to *CoCrMo* in the femoral component of a total knee replacement. Hip fractures in the elderly are dangerous injuries that result in increased morbidity and mortality, disability, and significant demand on medical resources. There is insufficient high-quality evidence to support the surgical strategy of hemiarthroplasty for the treatment of hip fractures [11].

Present study includes the *PLA* material for 3D printing of biomedical implants. Very few studies have reported data on *PLA* material used in hip implants. According to *Tol et al.* [11], a randomized clinical trial of 555 patients and an experiment of nature of 288 patients showed no difference in quality of life at six months post-injury between surgical interventions. Compared to *DLA*, *PLA* was associated with significantly higher rates of reoperations and dislocations. In 2020, *Obinna et al.*, [12] studied the 3D printing for hip implants.

Bhagia S. et al. [13] reviewed the *PLA* biocomposites containing biomass resources and characterized it as biodegradable, recyclable, and offering potential for biomass-derived fuel, electricity, heat and chemicals process and *FDM* printing. For *FDM* technology, *Prashant Anerao* [14] conducted a parametric study on the mechanical properties of biochar-reinforced *PLA* composite.

A comparative study and analysis of hearing aid housings printed from different biomaterials was conducted [15]. Using *ANSYS* explicit workbench, a comparative study of various polymer materials was conducted at five different drop impact test velocities. According to the study, *TPU* deformed to a maximum at all velocities, more than *PLA* or *ABS* [15]. *Dama et al.* [16] pointed out the suitability of the additive manufacturing process for reproducing design features. However, these materials are not suitable for 3D printing in a format that is accessible for conventional manufacturing processes. Fused deposition modeling (*FDM*) 3D printing, also called fused filament fabrication (*FFF*), is an additive manufacturing (*AM*) technique. Molten material is selectively applied along a predetermined route to build parts layer by layer. Thermoplastic polymers in the form of filaments are used to create the final physical products. *Daly et al.* conducted a parametric study and observed the effects of several 3D printing factors including

printing orientation, speed, and discretization method (layer by layer or filament) on warpage, residual stress, deflection, and mechanical behavior [17]. Sandanamsamy et al. examined the *FDM* printing process parameters on the tensile properties of *PLA* materials [18]. Meltem [19] studied the effects of *FDM* printing orientation on the tensile properties and printing time of a *PLA* part. The tensile strength decreased when the printing orientation of the parts was changed from horizontal to vertical and from 0° to 90° print angle (Figure 1). The tensile strength of the vertically printed part was 36 % lower than that of the horizontally printed part due to the load direction and failure mode.

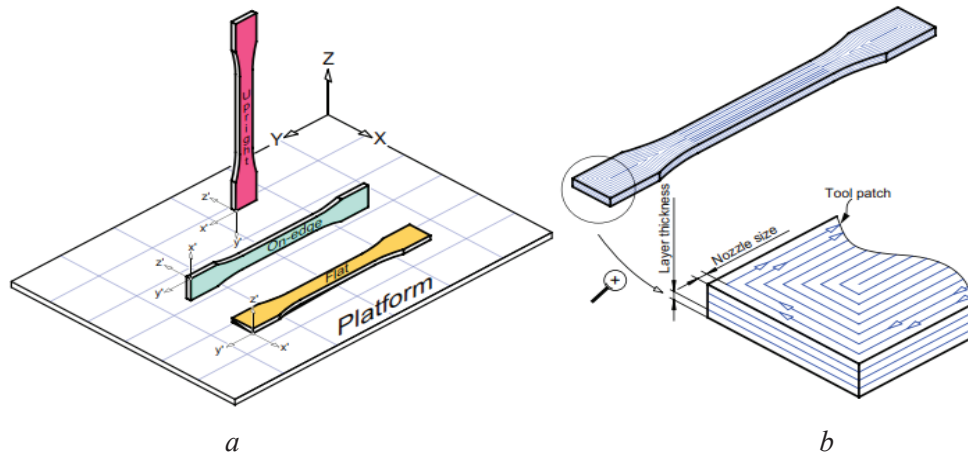


Fig. 1. *FDM* printing parameters:

a – printing orientations; *b* – raster direction angle equal to 0° and layer thickness.

Source: (Chacón et al. [20])

To ensure consistent and high-quality results, advanced manufacturing processes like fused deposition modeling (*FDM*) are being implemented in enterprises globally. For this reason, it is essential to understand how the various components interact and how it affects the quality of the final form. Wear behavior analysis of *PLA* parts has many applications in biomedicine, prosthetics, tissue engineering, and other industries.

The 3D printed *PLA* biomaterial needs to be thoroughly investigated for its potential use as a hip arthroplasty material through wear behavior and mechanical properties analysis.

The purpose of the work: This study examined the effect of printing orientation on the wear behavior of *PLA* biomaterial obtained by fused deposition modeling (*FDM*) under dry sliding friction conditions using the pin-on-disk (*SS 316*) scheme. In order to forecast the performance of both empirical and experimentally obtained models, the effect of sliding speed and load was taken into account. The grey relational analysis was used to determine the ideal parameters. The *FDM* 3D printing and wear testing equipment available at the Department of Mechanical Engineering, Vishwakarma Institute of Information Technology, Pune, Maharashtra, India was used in the study.

Further research is focused on the wear behavior study using composite materials to improve the wear rate performance [21–27]. 3D printing of composite biomaterial can be used to develop an implant with higher stability.

Investigation Technique

The pin-on-disc tribometer is a proven device for analyzing sliding wear and wear characteristics of the material. The working principle of the pin-on-disc tribometer is that the disk rotates at a constant speed while the pin remains stationary under a given load, and wear starts due to the relative motion between the pin and the disk. A linear variable differential transducer (*LVD*T) is used at the other end of the setup to record the displacement. This machine measures the coefficient of friction, friction force, wear rate,

temperature, wear volume etc. The pin-on-disk tribometer schematic diagram is shown in Fig. 2, *a*, and the device used for the experiments is shown in Fig. 2, *b*.

The machine operates at load range from 100 N to 800 N and rpm range from 20 rpm to 2,000 rpm. The measurement accuracy of the *LVDT* is $1 \pm 1 \%$ when measuring wear in μm and the smallest value is 1 μm . The test was carried out in accordance with *ASTM G 99*.

Fused deposition modeling (*FDM*) is one of the popular 3D printing techniques that uses thermoplastic polymers to create complex 3D structures. It allows for the clean and cost-effective creation of small functional parts. A wide variety of materials such as *PLA*, nylon, *ABS*, *PTFE* etc., with different process parameters can be used to print complex objects. During the printing process, thermoplastic filaments are melted and extruded through a heated nozzle, after which they are applied in a semi-solid state to a solid substrate. The schematic process diagram is shown in Fig. 3, *a*. The pins were printed using a *Flashforge Dreamer NX* 3D printer and a *PLA* material. Fig. 3, *b* shows a photograph of the 3D printer used to print the pins. All pins were produced at a fill density of 100 %, an extrusion temperature of 220 °C, a raster angle

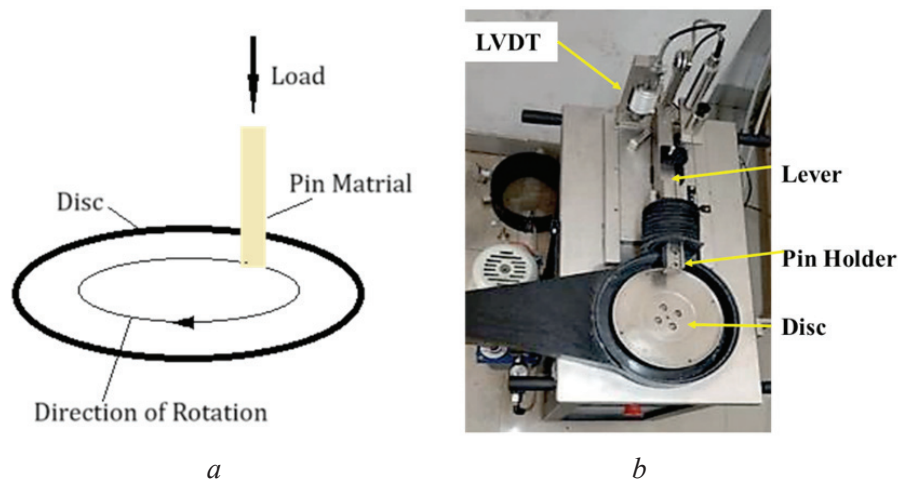


Fig. 2. Schematic diagram of the pin-on-disk tribometer (*a*); Experimental setup of the pin-on-disk tribometer (*b*)

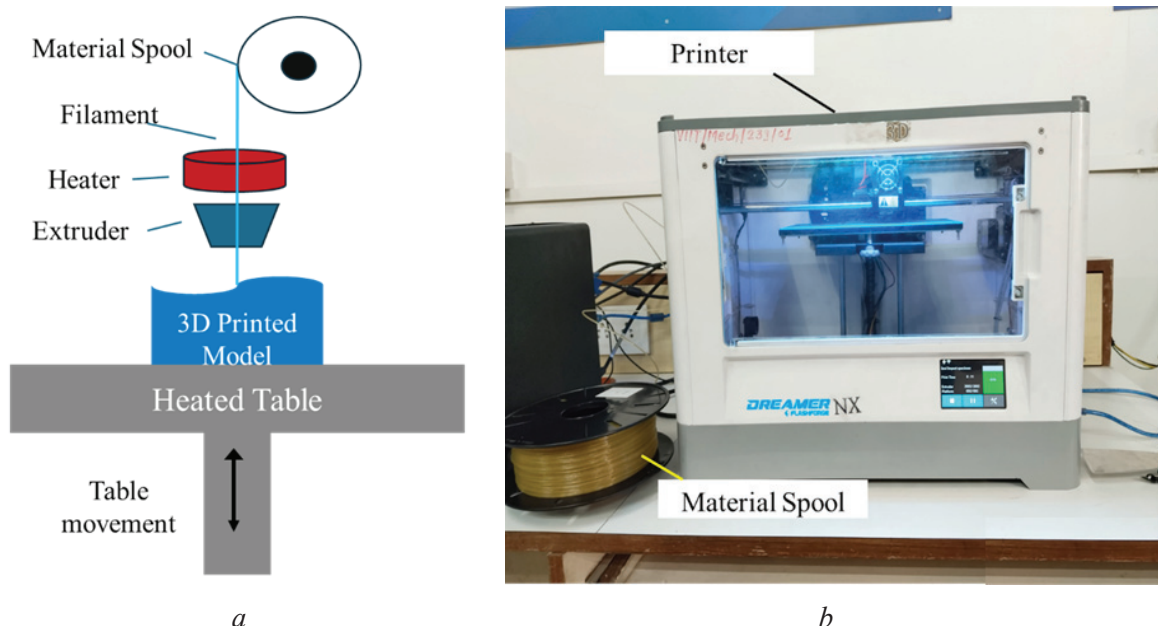


Fig. 3. FDM printing scheme (*a*) and FDM 3D printer (*Flashforge-Dreamer NX*) (*b*)

of 90°, and a layer thickness of 0.2 mm. According to the literature, these parameters are optimal. The test specimens were cylindrical *PLA* pins with a diameter of 8 mm and a length of 40 mm. These pins were printed at the printing orientation of 0°, 45° and 90°. *PLA* material is one of the popular filament materials used in *FDM* printing. *PLA* is easy to print and the printer can be easily adjusted to it.

The experiments were methodically designed to study the influence of input parameters on specific wear rate. Sliding velocities were obtained by selecting the track diameter on the disk and the corresponding rotation speed of the disk. *SS 316* stainless steel was chosen as the material for the disk. About 13 experiments were carried out for each printing orientation with a friction path of 4 kilometers. These were prepared based on the central compositional design (*CCD*) which is the effective design for experiments (*DOE*) for the *RSM* method. Table 1 shows the parameter values selected for the experiment.

Table 1

Values of parameters selected for the experiment

Parameters	Minimum value	Maximum value
Normal load (N)	400	800
Speed (rpm)	450	750
Sliding distance 4 km		

In this study, the grey relational analysis was used to optimize the parameters that ensure minimal sliding wear. The grey system theory presents the degree of grey correlation to describe the degree of correlation in the developing trends of different things or different factors. The greater the degree of grey correlation, the more similar the things are, and vice versa. This theory transforms a multiple response optimization problem into a single response optimization situation with the objective function of overall grey relational grade [27].

Methodology of grey analysis

The procedure for obtaining the solution of *GRA* optimization is given as follows:

Step 1. To identify input parameters that influence the multiple output variables.

Step 2. To select of *Taguchi* design matrix and conduct the experiments.

Step 3. To select quality characteristics for each output variable.

Step 4. To normalize all response variables (grey relational generation): the smaller-the-better normalization formula was used to transfer the original sequence to a comparable sequence and is given below.

$$x_i^*(k) = \frac{\max x_i^{(0)}(k) - x_i^{(0)}(k)}{\max x_i^{(0)}(k) - \min x_i^{(0)}(k)}.$$

Step 5. To determine the deviation Sequences, $\Delta 0i(k)$

The deviation sequence, $\Delta 0i(k)$ is the absolute difference between the reference sequence $x_0 \cdot(k)$ and the comparability sequence $x_i \cdot(k)$ after normalization. The value of $x_0 \cdot(k)$ was considered equal to 1.

$$\Delta 0i(k) = |x_0 \cdot(k) - x_i \cdot(k)|.$$

Step 6. To calculate the grey relational coefficient (*GRC*) for each output: grey relational coefficient. $\gamma(x_0(k), x_i(k))$

$$\gamma(x_0(k), x_i(k)) = \frac{\Delta \min + \zeta \Delta \max}{\Delta 0i(k) + \zeta \Delta \max}.$$

Step 7. To calculate the grey relational grade by mean value of *GRCs*: grey relational grade is an average sum of the grey relational coefficient, which is defined as follows:

$$\gamma(x_0, x_i) = \frac{1}{m} \sum_{k=1}^m \gamma(x_0(k), x_i(k)).$$

Step 8. To determine the optimal parameters.

Step 9. To predict the grey relational grade when setting optimal parameters.

Results and Discussion

The sliding wear study of *PLA* material on *SS 316* steel disc was carried out using a pin-on-disc friction machine. In this machine, a seesaw arrangement was made by attaching a rod to transfer the normal load to the pin by attaching weights to the other end. *LVDT* sensor was used to detect the change in displacement due to material wear. The rotation speed of the disk was varied by selecting an appropriate track diameter.

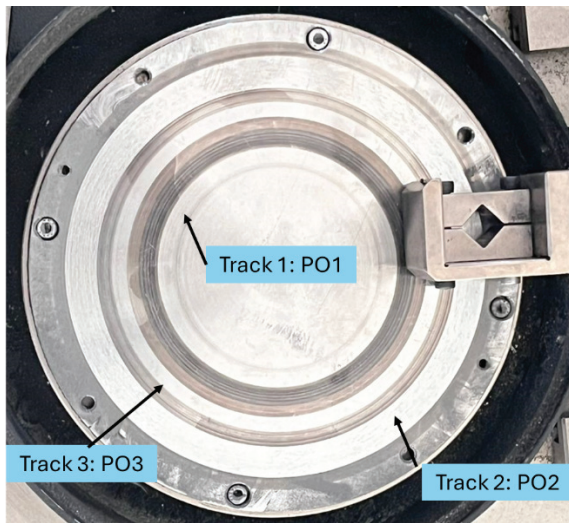


Fig. 4. Image of wear tracks of *FDM* printed pins on a *SS 316* stainless steel disc

The test was carried out on a 4 kilometer track distance (approx. 18 to 22 minutes). A control panel was attached to the machine, as well as a computer that displayed the speed, friction force and wear for the relevant processing parameters. *Windcom* software was used to show the variation in wear and friction force with respect to test time and track distance of 5 km. Figure 4 shows the wear track image of **PO1**, **PO2** and **PO3** formed on the *SS 316* disc.

The pins were manufactured using the *FDM* technology with printing orientations of 0°, 45° and 90°. Hereinafter, the pins manufactured with a printing orientation angle of 0°, 45° and 90° will be referred to as **PO1**, **PO2** and **PO3** respectively. The printing orientation of the pins in the form of a *CAD* model and in real printing is shown in Fig. 5, *a* and *b* respectively.

The experiments were performed according to *DOE* and the sliding wear was recorded for different values of normal load and sliding velocity. The experimental results along with the wear track images for all tests are summarized in Tables 2 and 3. All required environmental conditions were constant for all experimental tests. A mathematical equation based on the power law was used to predict the wear by considering the normal load (*N*) and speed (rpm) and is

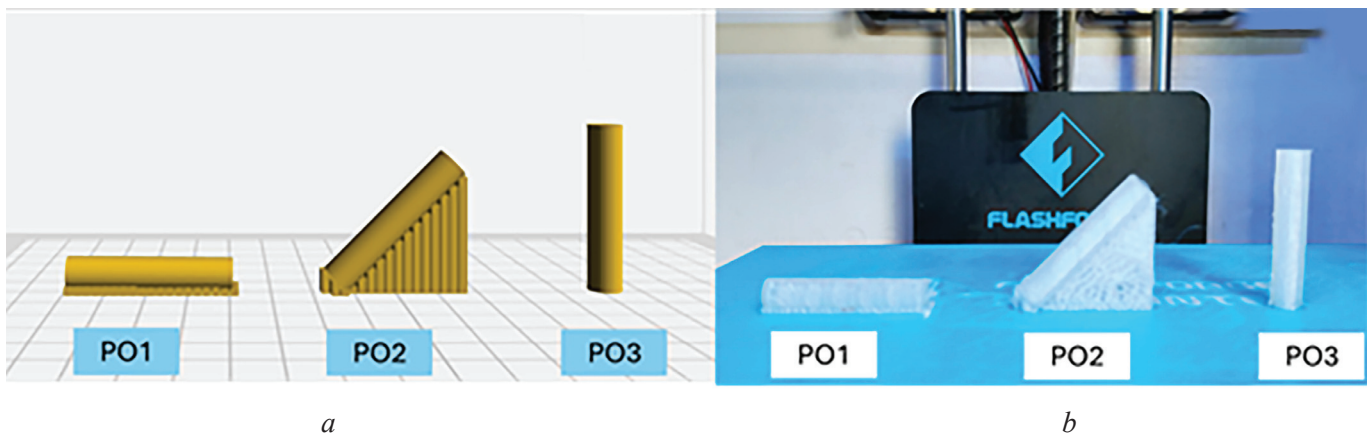


Fig. 5. 3D printing orientation:
a – *CAD* model; *b* – printed pins

Table 2



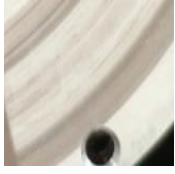



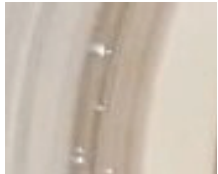



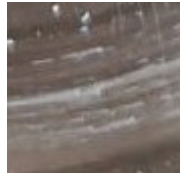

Experimental results of testing pins with different printing directions

Expt. No	Printing Orientation	Normal Load (N)	Speed (rpm)	Wear (μm)
1	<i>P01</i>	800	600	2,394
2	<i>P01</i>	600	451	2,178
3	<i>P01</i>	459	494	2,234
4	<i>P01</i>	600	600	2,398
5	<i>P01</i>	741	494	2,367
6	<i>P01</i>	741	706	2,429
7	<i>P01</i>	401	600	2,208
8	<i>P01</i>	600	600	2,320
9	<i>P01</i>	600	600	2,398
10	<i>P01</i>	600	600	2,367
11	<i>P01</i>	459	706	2,214
12	<i>P01</i>	600	750	2,391
13	<i>P01</i>	600	600	2,502
14	<i>P02</i>	800	600	3,293
15	<i>P02</i>	600	451	3,101
16	<i>P02</i>	459	494	2,877
17	<i>P02</i>	600	600	3,267
18	<i>P02</i>	741	494	3,012
19	<i>P02</i>	741	706	3,539
20	<i>P02</i>	401	600	2,896
21	<i>P02</i>	600	600	3,106
22	<i>P02</i>	600	600	3,148
23	<i>P02</i>	600	600	3,178
24	<i>P02</i>	459	706	3,273
25	<i>P02</i>	600	750	3,388
26	<i>P02</i>	600	600	3,147
27	<i>P03</i>	800	600	3,012
28	<i>P03</i>	600	451	2,683
29	<i>P03</i>	459	494	2,598
30	<i>P03</i>	600	600	2,796
31	<i>P03</i>	741	494	2,825
32	<i>P03</i>	741	706	3,201
33	<i>P03</i>	401	600	2,575
34	<i>P03</i>	600	600	2,867
35	<i>P03</i>	600	600	2,864
36	<i>P03</i>	600	600	2,854
37	<i>P03</i>	459	706	2,701
38	<i>P03</i>	600	750	3,056
39	<i>P03</i>	600	600	2,910

Table 3

Image of wear tracks for each test

Expt. No	Printing Orientation	Wear track image	Printing Orientation	Wear track image	Printing Orientation	Wear track image
1	<i>P01</i>		<i>P02</i>		<i>P03</i>	
2	<i>P01</i>		<i>P02</i>		<i>P03</i>	
3	<i>P01</i>		<i>P02</i>		<i>P03</i>	
4	<i>P01</i>		<i>P02</i>		<i>P03</i>	
5	<i>P01</i>		<i>P02</i>		<i>P03</i>	
6	<i>P01</i>		<i>P02</i>		<i>P03</i>	
7	<i>P01</i>		<i>P02</i>		<i>P03</i>	
8	<i>P01</i>		<i>P02</i>		<i>P03</i>	
9	<i>P01</i>		<i>P02</i>		<i>P03</i>	

Expt. No	Printing Orientation	Wear track image	Printing Orientation	Wear track image	Printing Orientation	Wear track image
10	PO1		PO2		PO3	
11	PO1		PO2		PO3	
12	PO1		PO2		PO3	
13	PO1		PO2		PO3	

given in Eq. 1. The power law is generally used to understand the influence of multiple input parameters on the output response.

$$W = a \cdot F_N^b \cdot S^c, \quad (1)$$

where F_N and S is normal load and speed respectively; a , b and c are the constants.

The values of these constants were determined for **PO1**, **PO2** and **PO3** using the experimental results. The mathematical equations for the *FDM* printed materials **PO1**, **PO2** and **PO3** are given in Table 4. *Data fit* software was used to determine the correlation between wear, normal load and speed.

The coefficient of correlation (R^2) was found to be 0.9244, 0.928 and 0.95 for **PO1**, **PO2** and **PO3**. This showed that the developed empirical equation can be used to determine the material wear under friction against a *SS 316* steel disc within the selected parameter. It is evident from the exponent of all equations that speed has a greater effect on wear compared to the normal load. 2D and 3D graphs were prepared to better understand the wear pattern. The loss of material is caused by wear, which eventually occurs due to the relative motion of two surfaces. Unlike friction, there is no energy loss. Polymers typically exhibit abrasive, adhesive, and fatigue wear mechanisms. Polymers tend to form a film that is transferred to the counterbody,

Table 4

Mathematical equations

Printing Orientation	Equation
PO1	$W = 432.8 \cdot F_N^{0.11} \cdot S^{0.16}$
PO2	$W = 234.9 \cdot F_N^{0.18} \cdot S^{0.23}$
PO3	$W = 123.5 \cdot F_N^{0.22} \cdot S^{0.27}$

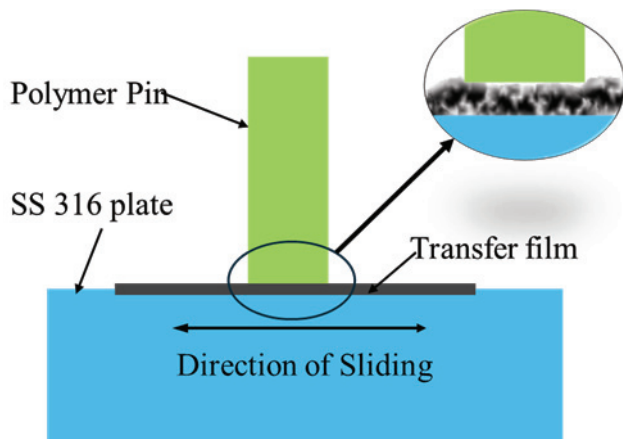


Fig. 6. Formation of the transfer film

which minimizes wear, so polymers are often chosen as a material for wearing parts. This is one of the important tribological phenomena. It is also known that when separation occurs inside the transfer film, it occurs between the film and the polymer rather than between the polymer and steel, so it acts as a protective layer that minimizes wear. The adhesive wear mechanism is one of the reasons for the development of the transfer film in polymer. A schematic diagram of the transfer film formation is shown in Fig. 6.

PLA is one of the popular materials because of its non-toxicity, biodegradability, biocompatibility and eco-friendliness. Additionally, since it is a 3D printing material, it is highly appreciated in biomedical

applications where there are relative motions between two surfaces (such as hip, knee and other joints). It has been reported in the literature that the printing orientation angle also plays an important role in the wear behavior of *PLA* material. In the present study, **PO1**, **PO2** and **PO3** pins were manufactured using additive technology with constant and optimized parameters reported in the literature so that the printing uniformity can be maintained. The effects of normal load and speed as well as printing angle on the wear behavior were studied. Figure 7, *a* and *b* show the effects of normal load and speed on the wear pattern of **PO1** pin (print orientation angle 0°).

A gradual increase in the wear was observed under normal load and variable speed. The minimum wear was recorded as $2,291 \mu\text{m}$ and the maximum was recorded as $2,523 \mu\text{m}$. From Fig. 7, *a* and *b*, it can be seen that the slope of the wear versus speed graph increased by almost 43 % compared with that of the normal load versus wear graph. This indicates that the speed has a prominent effect on the wear pattern. This was also evident from the exponent values of the equation (**PO1**) given in Table 4. As the speed increases, the vibrations in the system increase, which is an unfavorable condition for forming a stable transfer film. Fig. 8, *a* and *b* shows the effects of normal load and speed on the wear pattern for the **PO2** pin (print orientation angle of 45°).

The minimum wear of $2,948 \mu\text{m}$ and the maximum wear of $3,489 \mu\text{m}$ (Fig. 8, *a* and *b*) showed that the slope of the wear versus speed graph increased by almost 26 % compared to the slope of the wear versus normal load graph. The wear of **PO2** is greater compared to **PO1** in the considered cases. This was due to the improper bonding of the material at a printing orientation angle of 45° . A similar fact was also reported in the literature.

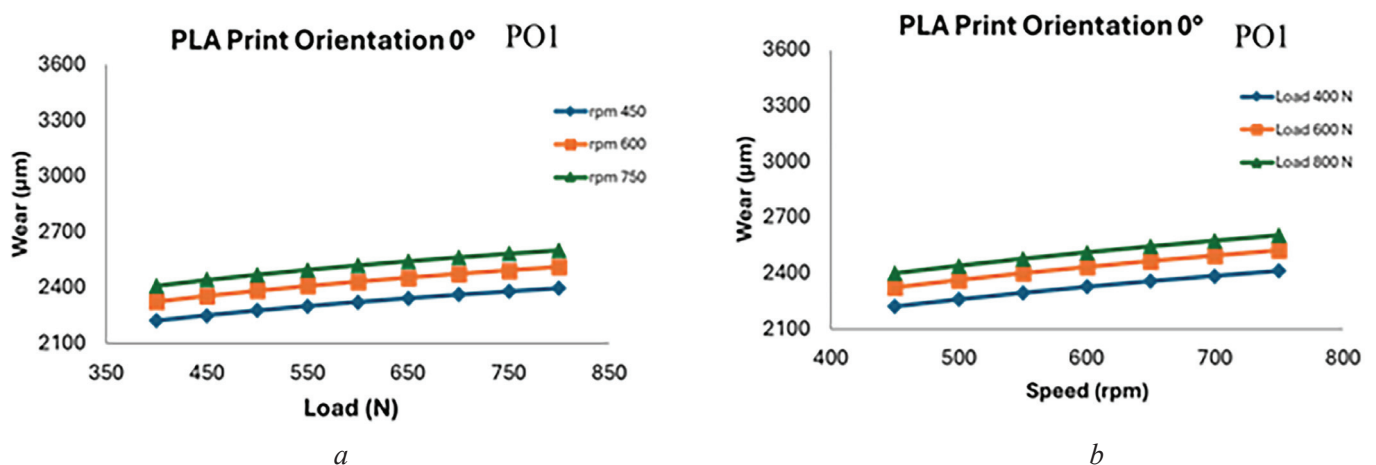


Fig. 7. Effect of normal load (*a*) and speed (*b*) on **PO1** wear

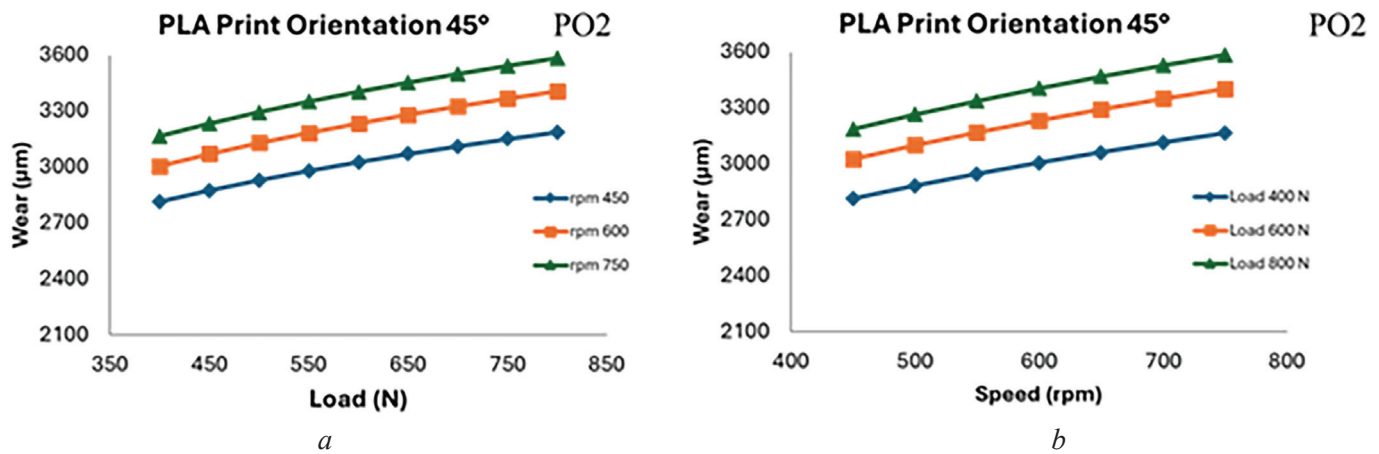


Fig. 8. Effect of normal load (a) and speed (b) on **PO2** wear

Figure 9, *a* and *b* shows the influence of normal load and speed on the wear pattern for **PO3** pin (printing orientation angle of 90°). A gradual increase in the wear was observed under normal load and variable speed. The minimum wear was recorded as 2,538 μm and the maximum wear was recorded as 3,106 μm. It is obvious from Figure 9, *a* and *b* that the slope of the wear versus speed graph increased by almost 21 % compared with that of the wear versus normal load graph. This indicates that the speed has a prominent effect on the wear pattern. A similar conclusion could be drawn from the exponent values of the equation (**PO1**) given in Table 4. It is observed from that above figures that **PO1** material shows lower wear followed by **PO3**. **PO2** exhibited the highest wear. The wear of FDM-printed PLA is greatly influenced by speed than normal load.

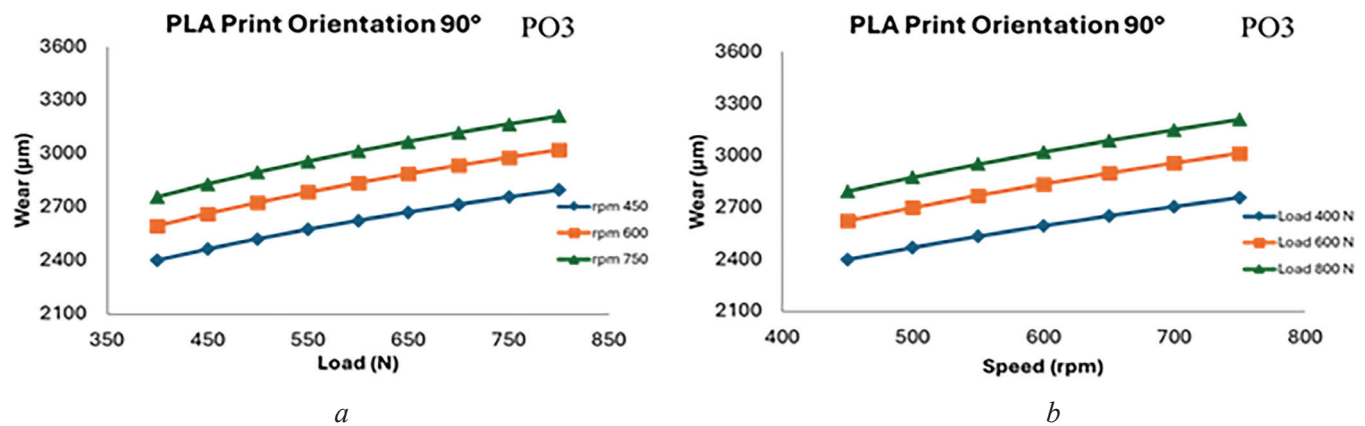


Fig. 9. Effect of normal load (a) and speed (b) on **PO3** wear

A comparative analysis of the wear of all specimens was performed by maintaining a constant speed and a constant load. The equation given in Table 4 was used to determine the wear at the corresponding constant load. The effect of normal load on the wear pattern of specimens **PO1**, **PO2** and **PO3** at a constant speed of 600 rpm and the effect of speed on the wear pattern of specimens **PO1**, **PO2** and **PO3** at a constant normal load of 600 N are shown in Figure 10, *a* and *b*, respectively. The load varied from 400 N to 800 N with a constant increment of 50 N.

It was observed that at constant speed of 600 rpm, **PO1** material exhibited lower wear compared to **PO2** and **PO3**. The lowest wear value for **PO1** was 2,328 μm, while the highest was 2,513 μm. For **PO2**, the lowest wear value was 3,008 μm, and the highest was 3,407 μm. For **PO3**, the lowest wear value was 2,595 μm, while the highest was 3,023 μm. The wear rate increased steadily, increasing by 1.08, 1.25, and 1.11 times with increasing load for **PO1**, **PO2**, and **PO3** specimens, respectively. **PO1** exhibited a more stable wear pattern compared to **PO2** and **PO3**. This was mainly due to the formation of a stable transfer

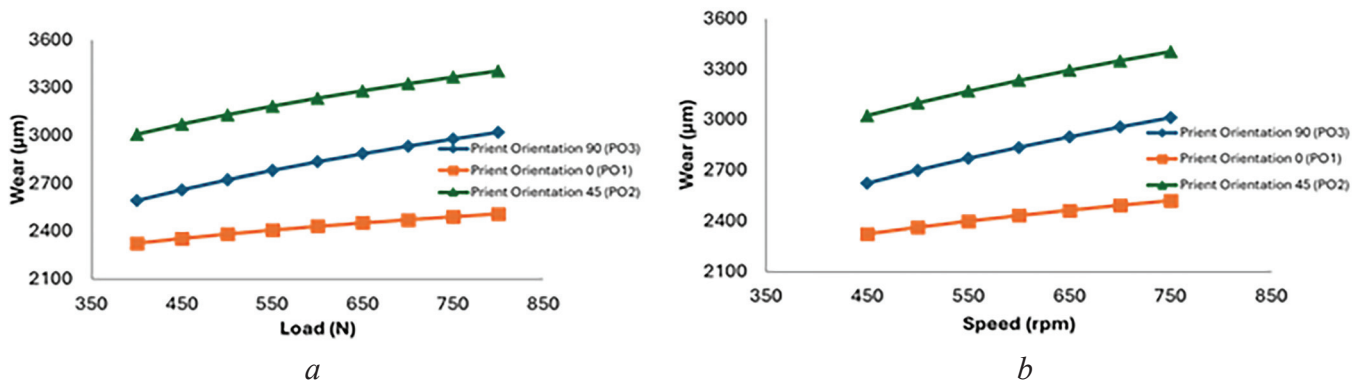


Fig. 10. Effect of normal load at constant speed of 600 rpm (a) and effect of speed at constant normal load of 600 N (b) on wear behavior of **PO1**, **PO2** and **PO3** specimens

film, which is clearly observed in the wear track images of the **PO1** material shown in Table 3. The better performance of the **PO1** was also attributed to the *FDM* printing orientation direction angle (i.e. 0°). In addition, the **PO1** material (as shown in Fig. 11) with a printing orientation angle of 0° showed excellent tensile and compressive strength, primarily because the printing orientation was aligned with the load application direction. In this position, the material layers have a constant thickness and a longer length in the **PO1** direction, which is likely to improve the bonding between the material layers, ultimately reducing wear.

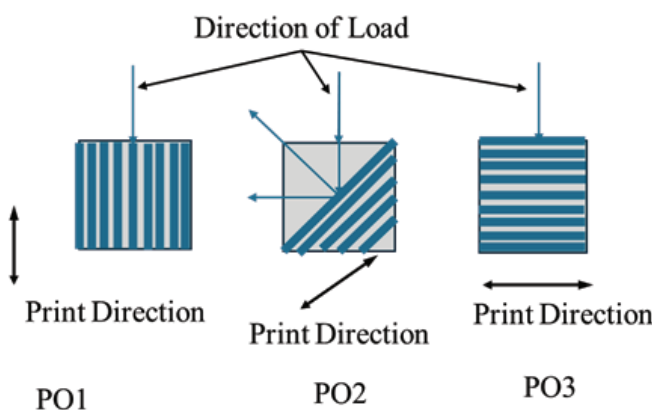


Fig. 11. Schematic diagram of the printing orientation and the direction of application of the normal load acting on the pin during testing

In addition, in the case of **PO2** and **PO3** materials, the printing orientation angle was 45° and normal to the loading direction. The layer adhesion is affected by the load and heat generated during operation [14]. As a result, a stable transfer film is not formed. This is also confirmed by the wear track images for **PO2** and **PO3** materials shown in Table 3. In the case of **PO2**, an uneven transfer film was observed, resulting in poor wear resistance. It should also be noted that the layer adhesion was poor in the specimens produced with a printing orientation angle of 30 – 60° [14, 26].

The schematic diagram of the printing orientation and direction of normal load acting on the pin during the test is shown in Fig. 11. The figure shows that in the case of **PO2** material, the load acting on the pin is further divided into two components. The horizontal component tries to weaken the bonding between the layers, causing vibration in the system; and because of this a stable transfer film is not formed, which leads to greater wear of **PO2**. In case of **PO2**, this phenomenon was not observed so the efficiency of **PO3** was higher than that of **PO2**. However, it should be noted that the bond strength is less in printing situation of **PO3** compared to **PO1**, so its efficiency is lower than that of **PO1**.

The values of normal load and speed in the equation from Table 4 for materials **PO1**, **PO2** and **PO3** indicate that wear is more dependent on normal load than on sliding speed. In order to have a clear understanding of the influence of the input parameters on wear, 3-D graphs of wear were plotted using the empirical equation given in Table 4 varying with normal load and sliding speed. The 3-D surface curves were plotted by varying the two process parameters simultaneously while keeping the third parameter constant in the middle value of the parameter ranges as shown in Table 1. The 3-D graphs reflecting the variation in the wear are shown in Fig. 12, a–c. Fig. 12, a, b, c depict the variation in the wear with the normal load and speed for **PO1**, **PO2** and **PO3**

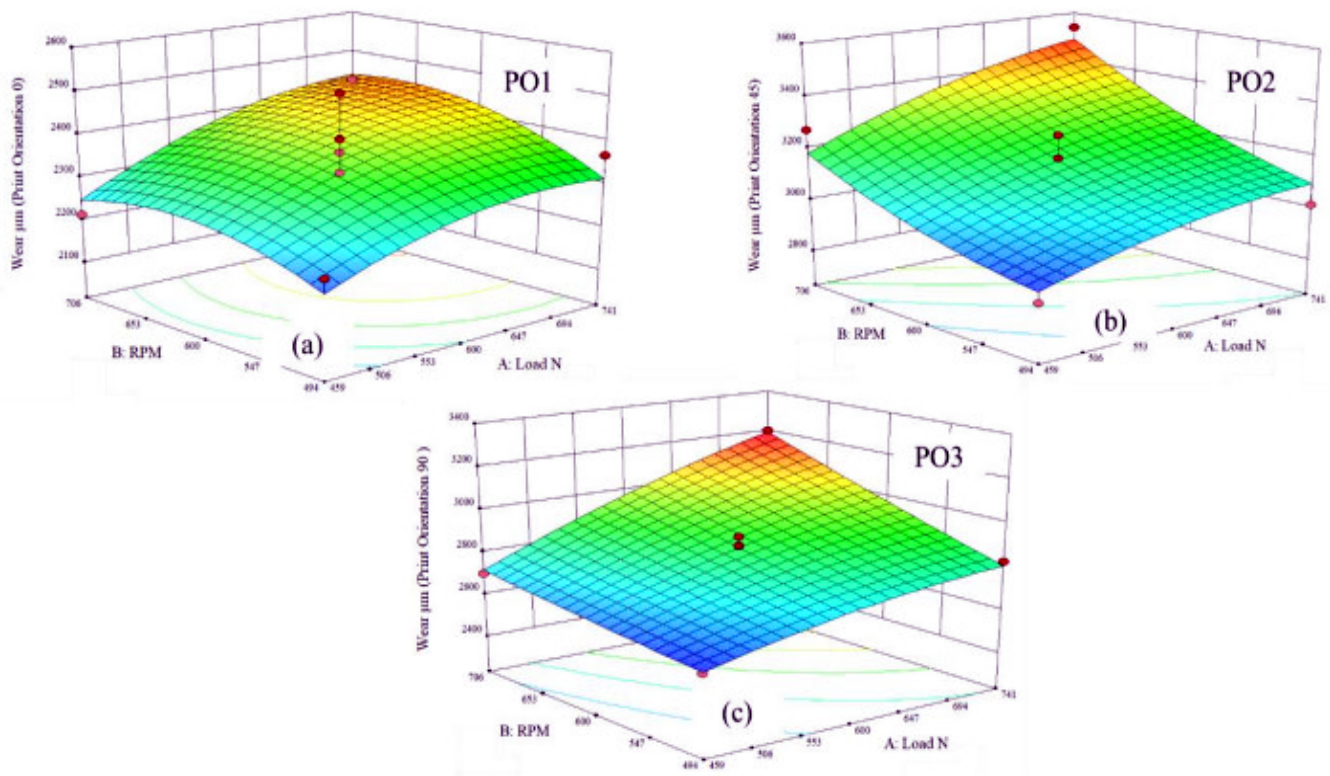


Fig. 12. 3-D graphs showing the change in wear depending on the normal load and rotation speed for:
a – **PO1**; b – **PO2** and c – **PO3**

respectively. The graphs are based on varying two process parameters while keeping the third parameter constant. The study revealed the influence of the interaction of process parameters and the printing orientation angle on the wear rate of *PLA* in a friction pair with *SS 316* stainless steel.

It is seen that the wear increases with the increase of speed and normal load. However, the increase in wear will become more noticeable at higher process parameters. The speed followed by normal load can be seen as most significant parameters affecting wear. This can also be confirmed by the higher exponent value for the speed followed by for load Table 4. This study finds that wear is prominently affected by speed, especially at higher values of normal load.

Grey relational analysis is the multi response optimization method that has been applied in the performance evaluation of various complex applications with limited information. It is widely used to measure the degree of relationship between sequences using gray relational grade. The procedure for *GRA* is explained above in the methodology. In the present study, the input factors were normal load and speed whereas *GRA* was conducted for the wear of **PO1**, **PO2** and **PO3** materials. The linear normalization of the experimental results for wear was based on the smaller-the-better approach. The experiments were conducted for different input parameters according to Table 1 for **PO1**, **PO2** and **PO3** specimen. A total of 39 experiments were conducted, of which 1–13 experiments were for **PO1**, 14–26 for **PO2** and the rest were for **PO3**. According to the procedure of *GRA* normalization of response ($xi(k)$), the deviation sequence ($\Delta 0i$) and the gray relation coefficient (*GRC*) for wear were determined. The values of $xi(k)$, $\Delta 0i$ and *GRC* for wear are shown in Table 5. A higher *GRC* indicates that the corresponding experimental conditions are optimal. Overall, **PO1** material showed excellent performance compared with **PO2** and **PO3**. However, **PO2** showed poor performance. The optimal values of normal load and speed were found to be 600 N and 451 rpm. *PLA*

Table 5

GRC values for all experiments

Expt. No	Orientation	Wear (μm)	$X_i(k)$	$0i$	GRC
1	PO1	2,394	0.84	0.16	0.758
2	PO1	2,178	1	0	1
3	PO1	2,234	0.96	0.04	0.926
4	PO1	2,398	0.84	0.16	0.758
5	PO1	2,367	0.86	0.14	0.781
6	PO1	2,429	0.82	0.18	0.735
7	PO1	2,208	0.98	0.02	0.962
8	PO1	2,320	0.9	0.1	0.833
9	PO1	2,398	0.84	0.16	0.758
10	PO1	2,367	0.86	0.14	0.781
11	PO1	2,214	0.97	0.03	0.943
12	PO1	2,391	0.84	0.16	0.758
13	PO1	2,502	0.76	0.24	0.676
14	PO2	3,293	0.18	0.82	0.379
15	PO2	3,101	0.32	0.68	0.424
16	PO2	2,877	0.49	0.51	0.495
17	PO2	3,267	0.2	0.8	0.385
18	PO2	3,012	0.39	0.61	0.45
19	PO2	3,539	0	1	0.333
20	PO2	2,896	0.47	0.53	0.485
21	PO2	3,106	0.32	0.68	0.424
22	PO2	3,148	0.29	0.71	0.413
23	PO2	3,178	0.27	0.73	0.407
24	PO2	3,273	0.2	0.8	0.385
25	PO2	3,388	0.11	0.89	0.36
26	PO2	3,147	0.29	0.71	0.413
27	PO3	3,012	0.39	0.61	0.45
28	PO3	2,683	0.63	0.37	0.575
29	PO3	2,598	0.69	0.31	0.617
30	PO3	2,796	0.55	0.45	0.526
31	PO3	2,825	0.52	0.48	0.51
32	PO3	3,201	0.25	0.75	0.4
33	PO3	2,575	0.71	0.29	0.633
34	PO3	2,867	0.49	0.51	0.495
35	PO3	2,864	0.5	0.5	0.5
36	PO3	2,854	0.5	0.5	0.5
37	PO3	2,701	0.62	0.38	0.568
38	PO3	3,056	0.35	0.65	0.435
39	PO3	2,910	0.46	0.54	0.481

components printed by *FDM* with a printing orientation angle of 0° are most suitable for parts susceptible to wear, followed by components with a printing orientation angle of 90° . Components manufactured with a printing orientation angle of 45° should not be applied.

Conclusion

This study demonstrates the wear characteristics of *PLA* material in a friction pair with SS 316 stainless steel to determine the optimal parameters. *FDM* printing was used to create the specimens with different printing orientation (0° , 45° , 90°). The experiments were conducted using the pin-on-disk friction scheme under different load and speed. Based on the experiment, a mathematical model was developed. In addition, grey relational analysis, a multi response optimization method, was used to determine optimal parameters. The uniqueness of this method is that it is used to evaluate the performance of various complex systems with insufficient information.

The following are the conclusions drawn from the study:

- The study of *PLA* material obtained by *FDM* with different printing orientation shows that horizontally printed pins have less wear than vertically printed ones. The greatest wear is characteristic of pins printed at an angle of 45° .
- It is noted that wear is significantly affected by speed followed by load. This is also confirmed by higher exponent values for speed and followed by load. A noticeable increase in wear is observed at higher process parameters.
- The *PLA* specimen printed by *FDM* with a printing orientation angle of 0° (***PO1***) exhibit less wear followed by specimen with printing orientation angle of 90° (***PO3***). This is mainly due to the high layer bonds strength along the printing orientation for ***PO1***. The specimen with a printing orientation angle of 45° (***PO2***) exhibit poor wear resistance due to thermal softening. The optimal parameters for ***PO1*** are found to be 600 N load and 451 rpm, which was determined using the multi variable grey relational analysis method.
- In the developed experimental mathematical model, the correlation coefficient (R^2) is found to be 0.9244, 0.928 and 0.95 for ***PO1***, ***PO2*** and ***PO3***. These models can be used to predict the wear of *FDM* printed *PLA* material in a friction pair with SS 316 stainless steel.
- The results of the study will be useful in 3D printing *PLA* biomaterial for hip joint application.

References

1. Ventola C.L. Medical applications for 3D printing: current and projected uses. *Pharmacy and Therapeutics Journal: Peer Review*, 2014, vol. 39 (10), pp. 704–711.
2. Gibson I., Rosen D., Stucker B. Direct digital manufacturing. *Additive Manufacturing Technologies*. 2nd ed. New York, Springer, 2015, pp. 375–397. DOI: 10.1007/978-1-4939-2113-3_16.
3. Patil N.A., Njuguna J., Kandasubramanian B. UHMWPE for biomedical applications: performance and functionalization. *European Polymer Journal*, 2020, vol. 125, p. 09529. DOI: 10.1016/j.eurpolymj.2020.109529.
4. Kurtz S.M. Primer on UHMWPE. *UHMWPE biomaterials handbook: ultra-high molecular weight polyethylene in total joint replacement and medical*. 3rd ed. Amsterdam, Elsevier, 2016, pp. 1–6.
5. Lewis G. Properties of crosslinked ultra-high-molecular-weight polyethylene. *Biomaterials*, 2001, vol. 22 (4), pp. 371–401. DOI: 10.1016/S0142-9612(00)00195-2.
6. Wang A., Essner A., Polineni V., Stark C., Dumbleton J. Lubrication and wear of ultra-high molecular weight polyethylene in total joint replacements. *Tribology International*, 1998, vol. 31, pp. 17–33. DOI: 10.1016/S0301-679X(98)00005-X.
7. Yousuf J.M., Mohsin A.A. Enhancing wear rate of high-density polyethylene (HDPE) by adding ceramic particles to propose an option for artificial hip joint liner. *IOP Conference Series: Materials Science and Engineering*, 2019, vol. 561, p. 012071. DOI: 10.1088/1757-899X/561/1/012071.
8. Orishimo K.F., Claus A.M., Sychterz C.J., Engh C.A. Relationship between polyethylene wear and osteolysis in hips with a second-generation porous-coated cementless cup after seven years of follow-up. *The Journal of Bone & Joint Surgery*, 2003, vol. 85 (6), pp. 1095–1099. DOI: 10.2106/00004623-200306000-00018.

9. Nabhan A., Sherif G., Abouzeid R., Taha M. Mechanical and tribological performance of HDPE matrix reinforced by hybrid Gr/TiO₂ NPs for hip joint replacement. *Journal of Functional Biomaterials*, 2023, vol. 14 (3), p. 140. DOI: 10.3390/jfb14030140.
10. Zhang X., Zhang T., Chen K., Xu H., Feng C., Zhang D. Wear mechanism and debris analysis of PEEK as an alternative to CoCrMo in the femoral component of total knee replacement. *Friction*, 2023, vol. 11, pp. 1845–1861. DOI: 10.1007/s40544-022-0700-z.
11. Tol M.C.J.M., Willigenburg N.W., Rasker A.J., Willems H.C., Gosens T., Heetveld M., Schotanus M.G.M., Eggen B., Kormos M., Pas S.L. van der, Vaart A. van der, Goslings J.C., Poolman R.W. Posterolateral or direct lateral surgical approach for hemiarthroplasty after a hip fracture: a randomized clinical trial alongside a natural experiment. *JAMA Network Open*, 2024, vol. 7 (1), p. e2350765. DOI: 10.1001/jamanetworkopen.2023.50765.
12. Obinna O., Stachurek I., Kandasubramanian B., Njuguna J. 3D printing for hip implant applications: a review. *Polymers (Basel)*, 2020, vol. 12 (11), p. 2682. DOI: 10.3390/polym12112682.
13. Bhagia S., Bornani K., Agarwal R., Satlewal A., Đurković J., Lagaña R., Bhagia M., Yoo C.G., Zhao X., Kunc V., Pu Y., Ozcan S., Ragauskas A.J. Critical review of FDM 3D printing of PLA biocomposites filled with biomass resources, characterization, biodegradability, upcycling and opportunities for biorefineries. *Applied Materials Today*, 2021, vol. 24, p. 101078. DOI: 10.1016/j.apmt.2021.101078.
14. Anerao P., Kulkarni A., Munde Y., Shinde A., Das O. Biochar reinforced PLA composite for fused deposition modelling (FDM): a parametric study on mechanical performance. *Composites, Part C: Open Access*, 2023, vol. 12, p. 100406. DOI: 10.1016/j.jcomc.2023.100406.
15. Gosavi A., Kulkarni A., Dama Y., Deshpande A., Jogi B. Comparative analysis of drop impact resistance for different polymer based materials used for hearing aid casing. *Materials Today: Proceedings*, 2022, vol. 49, pp. 2433–2441. DOI: 10.1016/j.matpr.2021.09.519.
16. Dama Y.B., Jogi B.F., Pawade R.S. Application of nonlinear analysis in evaluating additive manufacturing process for engineering design features: a study and recommendations. *Communications on Applied Nonlinear Analysis*, 2024, vol. 31 (1s), pp. 94–105. DOI: 10.52783/cana.v31.559.
17. Daly M., Tarfaoui M., Chihi M., Bouraoui C. FDM technology and the effect of printing parameters on the tensile strength of ABS parts. *The International Journal of Advanced Manufacturing Technology*, 2023, vol. 126 (11–12), pp. 5307–5323. DOI: 10.1007/s00170-023-11486-y.
18. Sandanamsamy L., Mogan J., Rajan K., Harun W.S.W., Ishak I., Romlay F.R.M., Samykano M., Kadirgama K. Effect of process parameter on tensile properties of FDM printed PLA. *Materials Today: Proceedings*, 2023. DOI: 10.1016/j.matpr.2023.03.217.
19. Eryildiz M. Effect of build orientation on mechanical behaviour and build time of FDM 3D-printed PLA parts: an experimental investigation. *European Mechanical Science*, 2021, vol. 5 (3), pp. 116–120. DOI: 10.26701/ems.881254.
20. Chacón J.M., Caminero M.A., García-Plaza E., Núñez P.J. Additive manufacturing of PLA structures using fused deposition modelling: effect of process parameters on mechanical properties and their optimal selection. *Materials & Design*, 2017, vol. 124, pp. 143–157. DOI: 10.1016/j.matdes.2017.03.065.
21. Kharate N., Anerao P., Kulkarni A., Abdullah M. Explainable AI techniques for comprehensive analysis of the relationship between process parameters and material properties in FDM-based 3D-printed biocomposites. *Journal of Manufacturing and Materials Processing*, 2024, vol. 8 (4), p. 171. DOI: 10.3390/jmmp8040171.
22. Paturkar A., Mache A., Deshpande A., Kulkarni A. Experimental investigation of dry sliding wear behaviour of jute/epoxy and jute/glass/epoxy hybrids using Taguchi approach. *Materials Today: Proceedings*, 2018, vol. 5 (11), pp. 23974–23983. DOI: 10.1016/j.matpr.2018.10.190.
23. Satkar A.R., Mache A., Kulkarni A. Numerical investigation on perforation resistance of glass-carbon/epoxy hybrid composite laminate under ballistic impact. *Materials Today: Proceedings*, 2022, vol. 59 (1), pp. 734–741. DOI: 10.1016/j.matpr.2021.12.464.
24. Kanitkar Y.M., Kulkarni A.P., Wangikar K.S. Investigation of flexural properties of glass-Kevlar hybrid composite. *European Journal of Engineering and Technology Research*, 2018, vol. 1, pp. 25–29. DOI: 10.24018/ejeng.2016.1.1.90.
25. Virpe K., Deshpande A., Kulkarni A. A review on tribological behavior of polymer composite impregnated with carbon fillers. *AIP Conference Proceedings*, 2020, vol. 2311 (1), p. 070030. DOI: 10.1063/5.0035408.
26. Chinchalikar S. Modeling of sliding wear characteristics of Polytetrafluoroethylene (PTFE) composite reinforced with carbon fiber against SS304. *Obrabotka metallov (tekhnologiya, oborudovanie, instrumenty) = Metal Working and Material Science*, 2022, vol. 24, no. 3, pp. 40–52. DOI: 10.17212/1994-6309-2022-24.3-40-52.



27. Pawade R.S., Joshi S.S. Multi-objective optimization of surface roughness and cutting forces in high-speed turning of Inconel 718 using Taguchi grey relational analysis (TGRA). *The International Journal of Advanced Manufacturing Technology*, 2011, vol. 56 (1–4), pp. 57–62. DOI: 10.1007/s00170-011-3183-z.

Conflicts of Interest

The authors declare no conflict of interest.

© 2024 The Authors. Published by Novosibirsk State Technical University. This is an open access article under the CC BY license (<http://creativecommons.org/licenses/by/4.0>).

